

## ARTICLE OPEN



# An advanced analytical approach to assess the long-term degradation of microplastics in the marine environment

Carbery Maddison<sup>1</sup>, C. I. Sathish<sup>2</sup>, Daggubati Lakshmi<sup>1</sup>, O'Connor Wayne<sup>3</sup> and Thava Palanisami<sup>1</sup>✉

Determining the hazards posed by microplastics (MPs, <5 mm) requires an understanding of plastic degradation processes when exposed to environmental weathering forces. However, despite their perceived risks, limited information exists on the natural weathering progression of microplastics in marine environments. Our findings from environmentally realistic conditions reveal that long-term marine weathering resulted in significant degradation of plastic surfaces and bulk-phases, which varied by time and plastic polymer type. Plastics displayed biofouling, and an altered surface morphology, thermal stability and chemical signature. Secondary micronanoplastics (MNPs, <1 µm) were formed from weathered plastic surfaces, supported by a significant reduction in the size of PCL and PVC pellets. Using real world data, we reveal that plastic surfaces can degrade at a rate of up to 469.73 µm per year, 12 times greater than previous estimates. Our time-series data contributes valuable information towards developing plastic specific risk assessment frameworks and future plastics policy.

*npj Materials Degradation* (2023)7:59; <https://doi.org/10.1038/s41529-023-00377-y>

## INTRODUCTION

Plastics are prolific environmental pollutants, with 79% of all plastic waste estimated to enter landfills and the environment<sup>1</sup>, emerging as a contaminant of growing concern. At the current rate of global plastic consumption, the mass of marine plastics is estimated to triple from 50 million tonnes (MT) in 2015 to 150 MT in 2025<sup>2,3</sup>, having significant implications for the health and ecosystem functioning of marine environments. Upon entering the environment, plastic is continuously subjected to weathering forces, generating microplastics (MPs, <5 mm in size) and potentially toxic by-products of the plastic degradation process<sup>4</sup>. Plastics continuously interact with their surroundings, leading to the transformation of exposed surfaces, while enhancing their toxic effects. Environmental factors such as heat, humidity, ultraviolet (UV) radiation, ozone, mechanical forces, chemicals and microorganisms contribute toward plastic degradation. Although the conditions required for the complete mineralization of plastics into non-toxic compounds are unlikely or naturally slow<sup>4,5</sup>, weathering is one of the most critical processes affecting the fate of marine plastics and is yet to be understood. Plastic degradation occurs several orders of magnitude slower in the marine environment than in terrestrial environments, due to the lower temperatures and UV intensity at the sea surface<sup>5</sup>. Here, plastics are in constant contact with water, dissolved chemical and biological compounds, and microbes, which can act as catalysts for the degradation process<sup>6</sup>.

Current knowledge of weathered plastics is mostly generated through ageing simulations and observations of field-collected plastics, which lack the necessary time-scale information. Artificial ageing studies provide evidence for the impacts of weathering processes, including flaking, cracking and changes in surface roughness<sup>7</sup>, as well as the release of microscopic plastic particles<sup>8</sup>. Only a few studies have explored the natural weathering behaviour of plastic materials<sup>9–11</sup>, however most are limited in their scope, focusing on few plastic polymer types and/or

relatively short time frames. In the absence of advanced analytical tools, previous studies have been unable to fully characterise the weathering behaviour of environmental plastics, preventing an in-depth understanding of their environmental risk. Changes in surface properties, including hydrophobicity/hydrophilicity, surface charge and roughness, may affect the adsorption of chemical contaminants, interactions with natural colloids and the presence of microbial biofilms<sup>12,13</sup>. At the same time, the bulk properties of plastics (e.g; degree of crystallinity, diffusivity and molecular structure) can profoundly influence the mechanical stability of plastic particles and chemical adsorption-desorption processes<sup>14</sup>.

Few exposure studies (<10%) employ environmentally weathered MPs, yet most (90%) conclude a significant effect of weathering on model organisms<sup>15</sup>. Much of the literature focuses on the effects of virgin plastic particles, resulting in a mismatch between environmental plastics and effect studies. Consequently, the effects of weathered plastics remain largely unknown. Therefore, further research is needed to develop our understanding of the weathering mechanisms of MPs and their potentially toxic effects in the environment.

Here, we present the most comprehensive investigation into the natural weathering behaviour of plastic materials in the marine environment and the first time-series data on the impacts of marine weathering forces on plastic materials to-date. Our study provides fundamental insights to; (i) gain an in-depth understanding of the impacts of natural marine weathering forces on the physicochemical properties of plastics, (ii) investigate time-dependant changes in the properties of marine plastics in-situ, and (iii) determine the role of weathering in moderating chemical (de) sorption. We anticipate that the outcomes of this research will progress our understanding of the behaviour, fate and potential hazards of marine plastics and contribute valuable information towards the development of an informed environmental risk assessment.

<sup>1</sup>Environmental Plastics Innovation Cluster (EPIC), Global Innovative Centre for Advanced Nanomaterials, The University of Newcastle, Callaghan, NSW, Australia. <sup>2</sup>College of Engineering, Science and Environment, The University of Newcastle, Callaghan, NSW, Australia. <sup>3</sup>Port Stephens Fisheries Institute, NSW Department of Primary Industries, Taylors Beach, NSW, Australia. ✉email: [Thava.palanisami@newcastle.edu.au](mailto:Thava.palanisami@newcastle.edu.au)

## RESULTS AND DISCUSSION

### Nano-scale examination of weathered plastic surfaces

The transformation of plastic surfaces by marine weathering forces can increase the surface roughness and number of sites available for chemical adsorption. Currently, it is unknown how plastic surfaces change over time, and how these changes may differ among plastic polymer types. Scanning electron microscopy (SEM) was used to visualise these nano-scale changes in plastic surfaces due to marine weathering forces. Initial observations revealed marine fauna and microorganisms occupied plastic surfaces in-situ. Surface adhesion, engulfment, and recruitment of macroinvertebrate organisms (e.g. ascidians, molluscs and crustaceans) to the surface of aged polyethylene terephthalate (PET) and expanded polystyrene (ePS) plastic particles were observed in the field (Supplementary Fig. 1), while marine microbes, diatoms, tube worms and epiphytes were visualised on aged ePS, linear low-density polyethylene (LLDPE), PET and polyvinyl chloride (PVC) via SEM (Supplementary Fig. 2). Of significant interest was the appearance of uniform craters on the surface of aged PET, which contained diverse microbial communities that may play a functional role in the degradation of xenobiotics, including plastic debris<sup>16</sup>. Consequently, we anticipate that these bubble-like structures were due to oxygen

production during microbial respiration or the presence of surfactants on the plastic surface during biodegradation. Several genera of marine bacteria, including *Arthrobacter* spp., *Pseudomonas* spp., and *Halomonas* spp., can produce and degrade marine biosurfactants and have been shown to colonise the surface of marine plastics in-situ<sup>16,17</sup>. These findings demonstrate that weathered PET provides a suitable habitat for marine microbes and adds to existing evidence supporting the biodegradation of marine plastics in-situ<sup>18,19</sup>.

Plastic-associated inorganic and organic matter (PIOM), including marine biofilms, dissolved compounds and particulates, is capable of sequestering toxic chemicals and pathogens to weathered plastic surfaces in marine environments<sup>10</sup>. Previously, we demonstrated that PIOM acted as a sink for metals, polyaromatic hydrocarbons (PAHs) and per- and polyfluoroalkyl substances (PFAS) on 10-year aged high-density polyethylene used in oyster aquaculture, which could potentially (de)sorb and detach from the plastic surface, posing a risk to resident marine biota. Here, we show that traces of PIOM were visible on weathered plastic surfaces after just one year (Fig. 1; SI Fig. 3), suggesting toxic chemicals and pathogens may accumulate on weathered plastics at least 10 times faster than previously reported. Visibly, aged polyaramid (PA) hosted the greatest

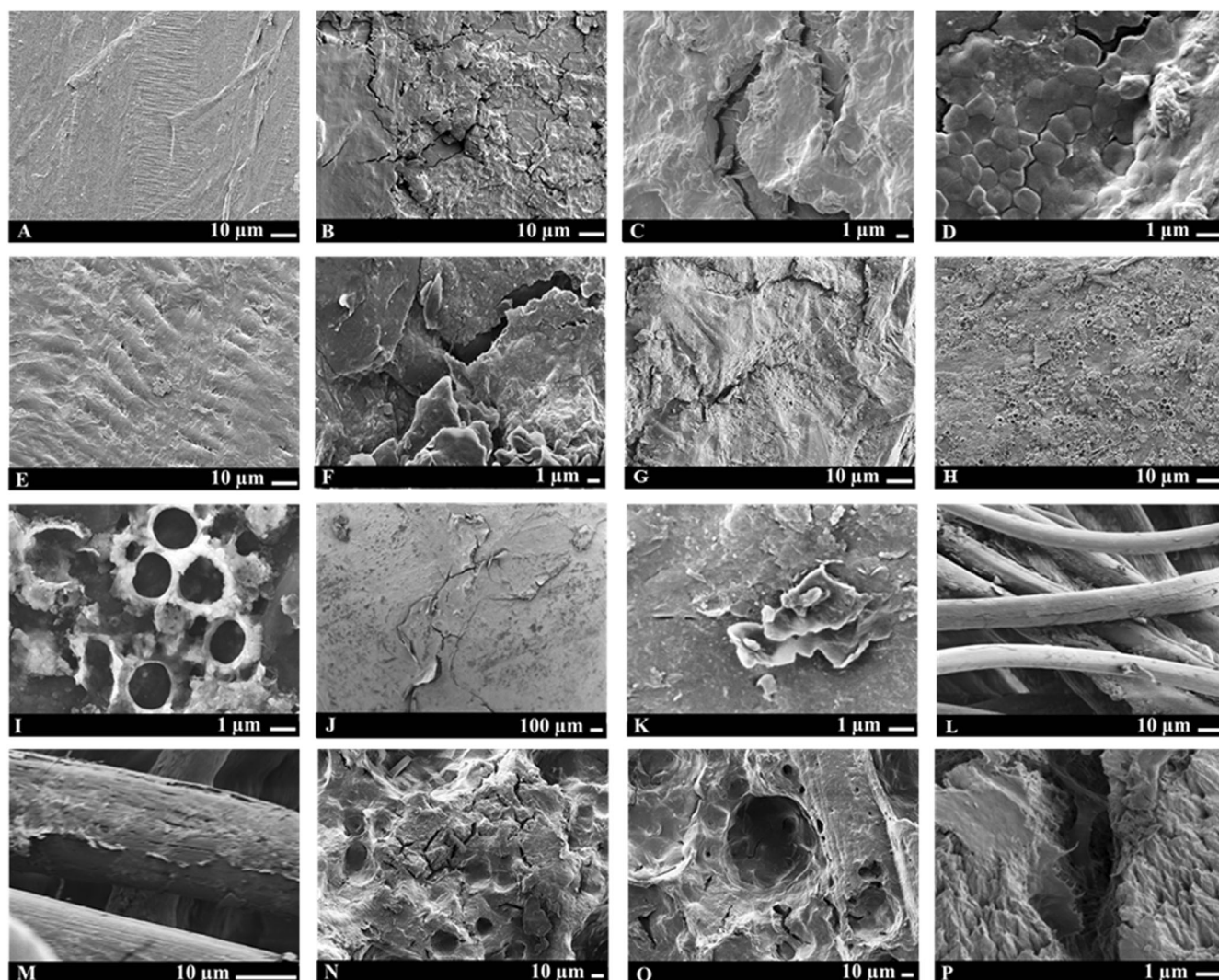


**Fig. 1** SEM micrographs of aged plastic surfaces following 12 months of exposure to marine weathering forces. Each panel displays the morphological features and artefacts observed on A–C LLDPE; D–F PP; G ePS; H–I PET; J, K PVC; L, M PA; and N–P PCL. Surface morphology of the virgin plastic surfaces are shown in Supplementary Fig. 3.



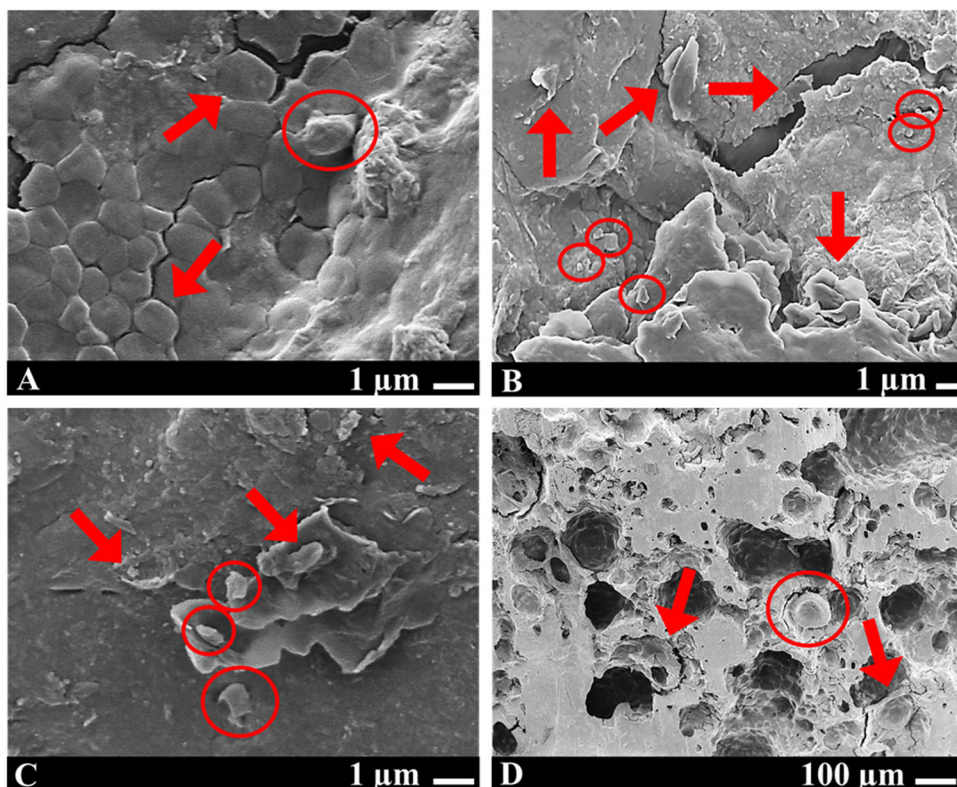


**Fig. 2 SEM micrographs showing the formation of micro-nano plastics on the surface of 12-month-aged plastic polymers.** The panels correspond to **A, B** PP, **C** PVC, and **D** PCL. Red arrows indicate the cracking and formation of small plastic particles on the plastic surface, whereas red circles indicate secondary micronanoplastics already formed on the weathered plastic surface.

amount of PIOM, which we attributed to the inherent hydrophilicity and high surface area of PA fibres, while a thin layer of PIOM covered the entire surface of weathered ePS. Due to the complex surface morphology of PA fibres and ePS foams, we suspect that the sample clean-up procedure did not completely remove entrapped (in)organic matter, which may have implications for the adsorption of chemical compounds and toxicity of plastic polymers in-situ.

The underlying surface of the weathered plastic materials exhibited an increase in surface roughness and heterogeneity due to flaking, pitting and cracking following 12 months of marine incubation (Fig. 1; Fig. 2 and Supplementary Fig. 3). Flaking, cracking and linear track marks were observed on the surface of aged LLDPE (Fig. 1A–C) and polypropylene (PP) (Fig. 1D–F), indicative of surface oxidation and deformation of the plastic surface, due to the diffusion of seawater into the internal free volume of low-density plastic polymers<sup>20,21</sup>. The web-like structures covering the surface of virgin ePS foams were replaced by creases and crevices, indicative of shrinking and compaction over time (Fig. 1G). Weathered PVC increased in surface roughness and displayed cracking and flaking of the pellet surface (Fig. 1J–K) due to extensive photo-oxidation<sup>22</sup>. Similarly, flaking and longitudinal cracks spanning the length of PA fibres were indicative of surface oxidation<sup>23</sup> (Fig. 1L–M). Transformation of polycaprolactone (PCL) surfaces by deep cracks, pits and holes provided evidence for advanced marine biodegradation in-situ<sup>19</sup> (Fig. 1N–P).

Fine micronanoplastics (MNPs, <1 μm) were seen cleaving and detaching from round cracks and deep fractures in PP, PVC and PCL plastic surfaces (Fig. 2), providing evidence for the formation and release of MNPs to the marine environment in-situ. Due to the uncontrolled nature of field studies however, we were unable to quantify release rates for MNPs during in-situ degradation. Previously, nanoparticle tracking analysis was used to investigate the degradation of PE, PP, PS, PET and polylactic acid (PLA) plastic

polymers during a 4-month ageing simulation<sup>8</sup>. The degradation process begun with photooxidation and chain scission at the polymer surface and resulted in increased surface area and the formation of MNPs (30 nm–60 μm in size). After 4 months, the concentration of MPs (2–60 μm) ranged from 2147 particles mL<sup>-1</sup> in the control to 92,465 particles mL<sup>-1</sup> for PS; large MNP (0.6–18 μm) concentrations ranged from 120,000 particles mL<sup>-1</sup> in the control to 11,600,000 for PLA; and small MNP (30–2000 nm) concentrations ranged from 20,000,000 particles mL<sup>-1</sup> in the control to 640,000,000 particles mL<sup>-1</sup> for PS. Therefore, our findings demonstrate the sheer number of MNPs that may be released to the marine environment during plastic degradation in-situ.

Plastic degradation is of significant concern due to fine plastic particle toxicity<sup>15</sup> and the release of plastic degradation products<sup>24</sup>. The small size and increased bioavailability of toxicologically relevant MNPs present a considerable risk to marine organisms and food webs<sup>25,26</sup>. Our findings will be helpful to characterise and quantify the release rates of plastic degradation products to determine the toxicological impacts of weathered plastics in real environments.

### Surface area analysis of weathered plastics

Weathering of semi-crystalline plastics results in heterogeneous surfaces due to the tendency for crystalline and amorphous regions of polymers to degrade at different rates<sup>27</sup>. As such, we expected there to be quantifiable differences in the specific surface area of aged plastic polymers, having implications for the adsorption of chemical contaminants from marine background waters. Weathered plastics increased in surface area following 12-months of marine incubation (virgin: 0.032–1.645 m<sup>2</sup> g<sup>-1</sup>; aged: 0.137–3.527 m<sup>2</sup> g<sup>-1</sup>) (Fig. 3). The greatest increase in BET surface area occurred for aged LLDPE (1265%), followed by PP (1202%)

and PCL plastic pellets (765%), with weathered PA exhibiting the lowest increase overall (114%). This was attributed to the strong, anti-weathering coatings (e.g. alkylid resins, silica nanoparticles etc) applied to polyamides to resist degradation and improve their environmental performance<sup>28</sup>. However, at the end of the incubation period, weathered PA yielded the highest overall specific surface area ( $3.527 \pm 0.001 \text{ m}^2 \text{ g}^{-1}$ ) owing to the high inherent surface area of fibrous materials which favours chemical adsorption<sup>29</sup>. Similarly, differences in the surface areas among plastic polymer types were reflective of differences in the microstructure of the virgin plastic surfaces and their ability to withstand environmental weathering forces. The net increase in the surface area of aged plastic materials confirmed the effect of weathering of the modification of plastic surfaces in-situ, as observed via SEM (Fig. 1). The  $\text{N}_2$  adsorption-desorption analysis provides further evidence that marine weathering processes altered the surface morphology of virgin plastic polymers following 12 months of marine ageing, increasing the specific surface area of the plastic materials by exposing the internal surface area.

### Time series analysis of changes in surface chemistry

The composition of the model virgin plastic polymers was confirmed via attenuated total reflectance fourier transform infrared spectroscopy (ATR-FTIR) and previously published data<sup>30,31</sup>. Weathered plastic surfaces demonstrated chemical signatures distinct from virgin plastic materials (Table 1 and Supplementary Table 1). Wide infrared (IR) bands appearing at  $3400 \text{ cm}^{-1}$  (O–H stretch),  $1645 \text{ cm}^{-1}$  (C=O, amide I) and  $1030 \text{ cm}^{-1}$  (C–O vibrations), corresponding to the presence of nitrogen and oxygen-containing functional groups, were attributed to surface oxidation, hydrolysis and remnants of microbial biofilms<sup>32,33</sup>. Fluctuations in the occurrence and intensity of IR peaks were attributed to the “reverse weathering” phenomenon,

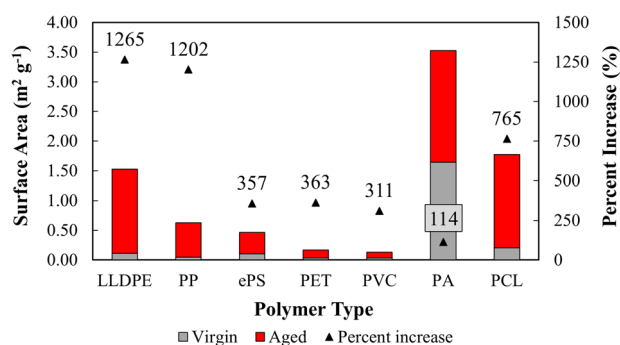


**Fig. 3** BET surface area ( $\text{m}^2 \text{ g}^{-1}$ ) of virgin (grey) and aged (red) plastic polymers incubated in the marine environment for 12 months. Percent increase (%) in the surface area of aged plastics is shown on the secondary y-axis, denoted by ▲.

whereby degradation of the plastic surface reveals previously unexposed regions of the polymer, generating spectra that more closely resembles the virgin material<sup>34</sup>. A decrease in the intensity of diagnostic IR peaks was due to the release of low molecular weight fragments and plastic degradation products to the marine environment via surface ablation, photo-oxidative- and biodegradation, and the end-chain scission of monomer units<sup>35,36</sup>. Consequently, aged plastics hosted dynamic surface environments, which varied by time and plastic type (refer Supplementary Fig. 4). Detailed information on changes in the surface chemistry of individual plastic polymers is provided in Supplementary Discussion 1.

Weathered plastics exhibited polymer-specific differences in ageing indices throughout time (aromatics>esters>olefins) (Fig. 4). Plastics containing aromatic compounds in their polymer chains (e.g., ePS and PA) ranked highest overall in terms of the degree of ageing, attributed to the strong absorption of benzene rings ( $\text{C}_6\text{H}_6$ ) in the UV range ( $\sim 300 \text{ nm}$ ). Additionally, the amide bond (RC(=O)NR/R') can be readily hydrolysed following prolonged exposure to acids and/or bases<sup>37</sup>, such as those naturally occurring in seawater (e.g.  $\text{H}_2\text{CO}_3$ , NaOH). Following 12 months of insitu ageing, we observed a significant increase in the hydroxyl index (HI > 10.0) and carbonyl index (CI  $\sim 7.0$ ) for weathered PA, attributed to the combined effects of UV radiation, enzymatic hydrolysis and the absorption of seawater<sup>38</sup>. Furthermore, the loss of anti-weathering coatings and extensive oxidation of the crystalline surface of PA fibres, evidenced by crack propagation under SEM (Fig. 2), resulted in exposure of the highly absorbent amorphous PA core<sup>38</sup>.

Polyesters (e.g., PET and PCL) and PVC were the next most susceptible plastic polymers to environmental weathering forces. Under marine conditions, photo-oxidation and hydrolytic cleavage of the ester bond (O–C=O) are considered major pathways for PET degradation, which is accelerated by the alkalinity (pH range  $\sim 8$ – $8.3$ ) and presence of hydroxide ions (i.e.,  $\text{OH}^-$ ) in seawater<sup>36,39</sup>. Additionally, enzymatic degradation of polyesters has been demonstrated in ambient seawater, due to the metabolic activity of esterases, cutinases and lipases<sup>40</sup>. Extensive hydrogen bonding resulting from hydrolytic degradation increases the number of hydrophilic end groups, increasing the hydrophilicity and polarity of PET materials in marine surface waters<sup>41</sup>. This change in surface chemistry can influence the interaction of weathered PET plastics with more polar compounds, such as metals and marine biofilms. PCL is considered relatively stable against abiotic hydrolysis due to its hydrophobicity and semi-crystalline nature, limiting the diffusion of water into the bulk phase<sup>42</sup>. Instead, PCL undergoes rapid biodegradation by microorganisms<sup>19,43</sup>, evidenced by deep fractures and pits via SEM (Fig. 1 and Fig. 2).

PVC degradation arises from its low stability and high sensitivity toward sunlight<sup>44</sup>. Ultra-violet light initiates dechlorination and HCl formation, resulting in an autocatalytic degradation process. As the backbone degrades into smaller fragments, metals, organotin stabilisers and plasticisers can readily migrate to the environment as they are not chemically bound to the polymer

**Table 1.** Summary of the main functional groups associated with weathered plastics in marine surface waters in this study<sup>65–67</sup>.

Functional group	Bond structure	Wavenumber ( $\text{cm}^{-1}$ )	Weathering factor	Plastic type
Hydroxyl	O–H	3100–3700	Surface oxidation, moisture	LLDPE, PP, ePS, PET, PVC, PA, PCL
Carbonyl	C=O	1600–1800	Surface oxidation, biogenic sources	LLDPE, PA, PCL
Amide (I)	C=O with $-\text{NH}_2$	1650–1580	Biogenic sources	PP, PVC, PA, PCL
Alkene, carbon double bond	C=C	1600–1680	Biogenic sources	LLDPE, PP, PVC, PA, PCL
Amine (II)	$-\text{NHR}$	1480–1580	Biogenic sources	PVC, PA, PCL
Amine (III)	$-\text{NHRR}'$	1200–1280	Biogenic sources	PVC, PA, PCL
Carbon-oxygen	C–O	1000–1200	Surface oxidation, biogenic sources	LLDPE, PP, ePS, PVC, PCL
Other (e.g., halogens)	e.g., C–F, $-\text{Cl}$ , $-\text{Br}$ , $-\text{I}$	1150–500	Ion adsorption	PP, ePS, PET, PVC, PA,

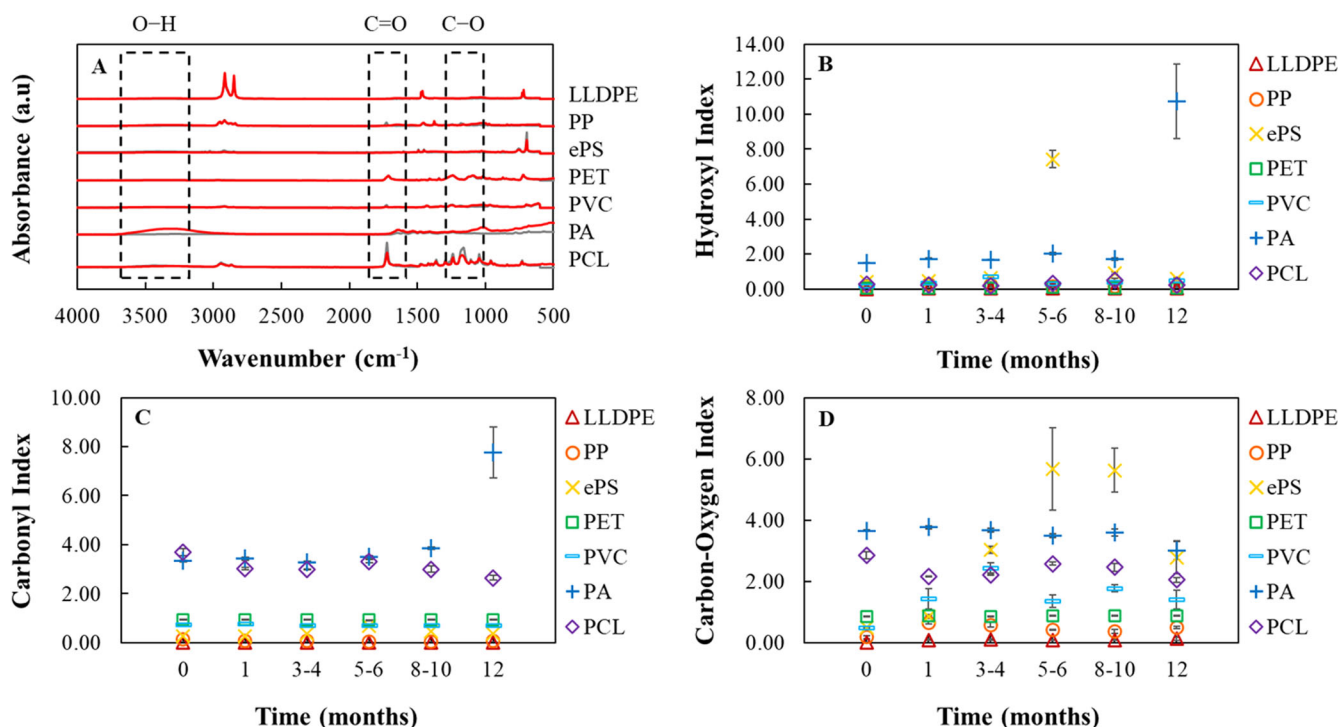


**Fig. 4 FTIR ageing indices for weathered plastic polymers.** **A** The position of the hydroxyl (O–H, 3100–3700  $\text{cm}^{-1}$ ), carbonyl (C=O, 1600–1800  $\text{cm}^{-1}$ ) and carbon–oxygen (C–O, 1000–1200  $\text{cm}^{-1}$ ) bands used to calculate the **B** hydroxyl index, **C** carbonyl index and **D** carbon–oxygen index for 12 month-aged plastics over time.

matrix<sup>36</sup>. Since halogens and chlorines increase the resistance of polymers to aerobic biodegradation, abiotic degradation is considered the primary pathway of degradation in PVC. However, the combined impact of (a)biotic weathering forces can alter the mechanical properties of PVC<sup>44</sup>, resulting in an overall decrease in molecular weight and migration of toxic PVC MNPs to the environment.

Aliphatic polyolefins (e.g., PP and LLDPE) appeared least affected by environmental weathering forces. Their high stability can be attributed to antioxidants (e.g., phenolic antioxidants, organophosphorus compounds and hindered amines) and light stabilisers (e.g., benzotriazole UV stabilizers and octabenzene) designed to slow the ageing process<sup>45</sup>, as well as a lack of reactive functional groups in the polymer backbone<sup>4</sup>. However, chromophoric compounds (e.g., solvents, catalyst residues, hydroperoxides, unsaturated double bonds and carbonyl groups) introduced during manufacturing and ageing processes may facilitate slow environmental degradation<sup>46,47</sup>. During the ageing of PP, an increase in the band intensities at 1645  $\text{cm}^{-1}$  and 1035  $\text{cm}^{-1}$  indicated an increase in elemental carbon, nitrogen and oxygen due to surface oxidation and the presence of PIOM. We attributed the appearance of new peaks below 800  $\text{cm}^{-1}$  to the adsorption of metal halides (e.g., C–F, –Cl, –Br and –I) present in seawater, facilitated by the charged nature of marine biofilms and PIOM<sup>48,49</sup>.

Overall, non-linear changes observed in the ageing indices for plastics weathered in the natural marine environment support the findings for PE and PP plastics aged over the long-term ex-situ<sup>34</sup>. Furthermore, the relatively low levels of surface oxidation observed for some weathered plastic polymers suggests a shielding effect of PIOM and warrants further investigation. Nevertheless, we demonstrate that ageing indices provide useful semi-quantitative information regarding the extent of surface degradation for plastics weathered in marine environments in situ.

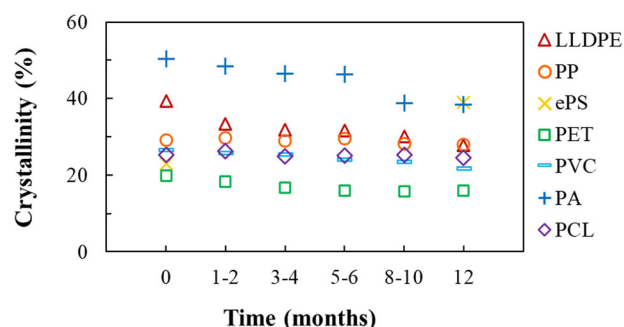


**Fig. 5** Differences in percent crystallinity (%) of the model plastic polymers over 12 months incubation in marine surface waters.

### Structural changes in weathered plastic polymers

Crystallinity is an important property of polymers as it affects the density and water permeability of plastic materials, thus influencing their degradation and environmental behaviour<sup>50</sup>. Polymers are the building blocks of large chain monomers with a higher degree of polymerization. These polymers behave as crystalline materials when the molecular chains are orderly arranged in 3D symmetry and form amorphous polymers when randomly oriented. X-ray diffraction (XRD) is a simple and most effective way to quantify the degradation of polymers by computing the change in crystalline to amorphous nature. XRD analysis revealed that the model plastic polymers were representative of semi-crystalline and amorphous materials, with crystallinity following the order; PA > LLDPE > PP > PVC > PCL > ePS > PET (Fig. 5). We note that some plastics deviated from their reported crystalline content, attributed to differences in the mass number, degree of chain branching and thermal history among batches of the model plastic polymers<sup>27</sup>.



Weathered plastic polymers demonstrated a decrease in crystallinity (virgin: 19.94–50.32%; aged: 15.96–38.35%), with the exception of ePS. This was attributed to the degradation of crystalline lamellae and increased lamellar spacing following prolonged exposure to UV radiation, immersion in seawater and colonisation by microbes. Time-dependant fluctuations in the crystalline content of plastic surfaces can be attributed to physicochemical degradation and reverse weathering processes (Supplementary Fig. 5). Physical ageing can increase the crystal structure and overall crystallinity of plastic materials, while chemical ageing initiates the breakage of molecular bonds, resulting in chain scission and a decrease in crystalline regions<sup>51</sup>. For example, aged PP and PCL fluctuated in crystallinity over the 12-month weathering period, due to increasing fractional crystallinity<sup>27</sup>, surface degradation and the shedding of small MNPs, exposing the underlying amorphous core.

New diffraction peaks were evident for some plastic polymers, indicative of enhanced crystal structure (Supplementary Fig. 5 and Supplementary Table 2). However, given the overall decline in polymer crystallinity, and the inability of amorphous polymers to be crystallised, we attribute these peaks to the adsorption of crystalline moieties over the surface of aged plastic materials. For example, we anticipate that the dramatic increase in crystallinity of 12-month aged ePS was a result of its high affinity for dissolved metal(loid)s in seawater<sup>52</sup>. Similarly, the appearance of new diffraction peaks at a  $2\theta$  value of  $26.5^\circ$  for weathered ePS and PA, corresponded to the cubic phase of  $\text{SiO}_2$ <sup>53</sup>, which we credited to siliceous deposits within the PIOM. Finally, the appearance of two new diffraction peaks at  $\sim 44^\circ$  and  $50^\circ$  for weathered PA support the timeframe of succession of marine microbial biofilms<sup>54</sup> which can enhance (in)organic chemical adsorption.

The crystallinity of plastic materials has significant implications for the formation and release of MNPs to the environment. For example, crystalline regions, represented by flaking, cracking and fracturing of weathered plastic surfaces, are hotspots for the formation of secondary MNPs<sup>27</sup> (Fig. 2). In contrast, an increase in amorphous domains due to degradation of crystalline lamellae can increase the adsorption of hydrophobic organic compounds, enhancing the vector potential and toxicity of plastic particles to marine biota<sup>9,14,55</sup>. Therefore, we demonstrate that weathered plastics present an increased risk to marine biota due to the formation of small plastic particles and the release of plastic degradation products to the surrounding seawater.

### Thermal properties and stability of weathered microplastics

Thermal gravimetric analysis (TGA) provides an accurate measurement of changes in the thermal properties of microplastics during the degradation process. Here, TGA analysis revealed a slight decrease in the onset of thermal decomposition for 12-month-aged ePS, PVC and PA (Supplementary Fig. 6C–E), indicative of a

decrease in the thermal stability of weathered plastic polymers following exposure to marine weathering forces. Owing to the high thermal and chemical stability of ePS, the initial decrease in weight was attributed to the thermal properties of adsorbed substances. For aged PVC, a slight decrease in the decomposition temperature corresponding to the onset of dechlorination ( $\sim 300^\circ\text{C}$ )<sup>56,57</sup> was attributed to the fact that dechlorination had already begun in-situ. Similarly, a decrease in the thermal decomposition temperature for weathered PA was attributed to the combined effects of UV radiation and sea water absorption<sup>38</sup>.

The thermal properties of PIOM were thought to influence the weight loss curves for weathered plastic materials, providing evidence for the shielding effects of PIOM. For example, SEM analysis indicated greater levels of PIOM were associated with weathered ePS and PA surfaces, due to the complex surface morphology of the virgin materials (refer Supplementary Fig. 3). Consequently, thermal analysis of weathered samples revealed an increase in the heat flow capacity for aged ePS and PA, attributed to the enhanced thermal properties of the inorganic fraction of PIOM, and increased residual ash content for aged ePS samples (Supplementary Fig. 6C, E). Further information on the thermal properties and decomposition behaviour of virgin and 12-month-aged plastic polymers are detailed in Supplementary Discussion 2.

Differential scanning calorimetry (DSC) was used to gauge the extent of plastic degradation due to marine weathering by measuring deviations in the heat capacity and phase transitions of virgin and 12-month-aged plastic polymers. Analysis of the heat flow curves indicated that aged plastics generally absorbed more heat than virgin materials (Fig. 6; Supplementary Fig. 6), due to the thermal properties of the PIOM. This was most pronounced in weathered ePS, which displayed an increase of  $4^\circ\text{C}$  in its thermal decomposition temperature (Supplementary Fig. 6C). The DSC heat flow curve for aged PET revealed that  $T_m$  decreased by  $8^\circ\text{C}$  following 12 months of natural marine ageing, indicating decreased thermal stability for weathered PET (Fig. 6). This was attributed to the degradation of ester groups, carbon double bonds and bulky side groups in the polymer chain, as well as cross-linking processes<sup>58</sup>. Finally, the heat flow curve for PCL confirmed that the onset of  $T_m$  commenced at  $\sim 40^\circ\text{C}$  for the model PCL, providing further evidence to support the degradation of PCL in marine surface waters, as indicated by XRD (refer Supplementary Fig. 5).

### Revisiting the crystallinity of plastic materials

The degradation of plastic materials is commonly associated with an increase in the crystallinity of polymers, evidenced via crack propagation, increased brittleness and the release of small plastic particles to the environment<sup>34,59,60</sup>. However, limited field data exists to support this phenomenon. The primary site of photo-oxidation of polymers occurs in the amorphous region, as oxygen

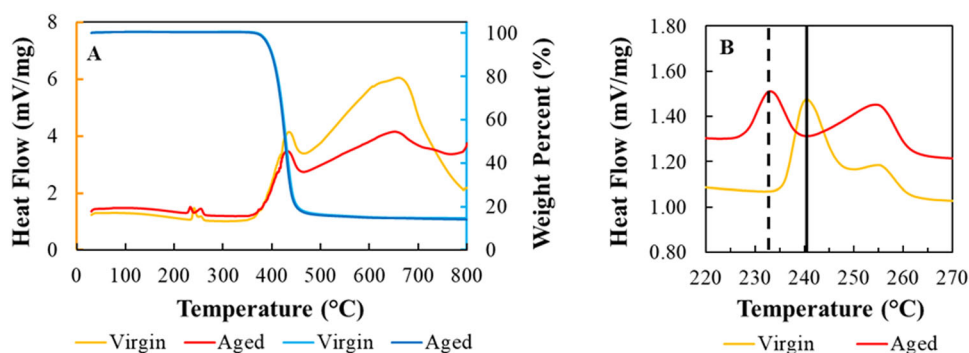


**Fig. 6** Thermal analysis of virgin and 12-month aged PET. **A** The TGA–DSC curves of virgin versus aged PET. **B** A decrease in the melting and recrystallization temperature of long-term weathered PET (solid line to dashed line).

permeability is reduced in the crystalline fraction<sup>27</sup>. As such, the amorphous regions of polymers are preferentially degraded during weathering, which can increase fractional crystallinity at the polymer surface and result in chemi-crystallisation. However, degradation of crystalline lamellae and increased cross-linking behaviour may facilitate a reduction in the crystallinity of long-term aged microplastics.

Our results indicate that prolonged marine weathering results in decreased crystallinity of semi-crystalline polymers. However, as limited data exists with which to evaluate our findings, we compared the use of several analytical techniques to approximate the true crystallinity values. Detailed results of the analyses can be found in the Supplementary Information (Supplementary Fig. 7). Overall, X-ray diffraction, spectroscopy and thermal analysis agreed that the crystalline behaviour of long-term weathered MPs decreased over time (Supplementary Fig. 7). Differences in crystallinity values within plastic polymer types were attributed to differences in the analytical approach among instruments. For example, DSC calculations are based on the thermal properties of the entire sample mass and are therefore less likely to reflect surface changes<sup>61</sup>, whereas XRD and FTIR provide information on the molecular and chemical structure of the surface region, respectively. Consequently, we can consider penetration depth of DSC analysis as far greater than that of high angle XRD or ATR-FTIR analysis (both of which are only a few microns and depend on the angle of incidence, material density and thickness of the sample). Subsequently, penetration depth follows the order DSC > XRD > FTIR, which can be considered inversely proportionate to the values obtained for the crystallinity of plastic materials in this study (FTIR > XRD > DSC) (Supplementary Fig. 7). In this regard, we recommend that future research into the crystalline behaviour of weathered plastics consider the sample region of interest when selecting the appropriate analytical technique. Furthermore, crystallinity results calculated from IR spectroscopy may be influenced by the presence of marine biofilms on weathered plastic surfaces and must therefore be interpreted with caution. Nevertheless, these complementary techniques agree that the crystallinity of weathered plastics largely decreases over time and confirms that the degradation of plastic materials is initiated by weathering of the surface, which is highly relevant for understanding the formation of secondary MNPs and contaminant adsorption-desorption processes.

### Cumulative effects of weathering on plastic particle size

The cumulative impacts of the surface and bulk-phase degradation of long-term weathered microplastics were expressed as a function of particle size (Supplementary Fig. 8). Following 12 months of marine incubation, we found that the mean diameter of LLDPE increased by 21.36 % (virgin:  $3674.05 \pm 72.25 \mu\text{m}$ ; aged:  $4459.00 \pm 49.31 \mu\text{m}$ ;  $t(7) = -8.974$ ,  $p < 0.001$ ), suggesting a net increase in pellet volume. This finding was supported by a substantial increase in the BET surface area of 12-month aged LLDPE (1265%), as shown in Fig. 3. We offer two possible

explanations for this; firstly, the high water vapour barrier properties of LLDPE (water absorption value: 0.005–0.01%) (ASTM D570-98(2010)e1) may have been compromised following long-term immersion in seawater, leading to increased water absorption and the subsequent swelling of LLDPE pellets<sup>62</sup>. However, due to the low hydroxyl index derived for LLDPE over the course of ageing (Fig. 4B), the unravelling of crystalline lamellae and a subsequent decrease in the crystal structure (Fig. 5) were considered driving factors for the increase in particle size.

The mean diameter of PCL and PVC decreased by 13.46%, (virgin:  $3489.53 \pm 35.96 \mu\text{m}$ ; aged:  $3019.80 \pm 43.82 \mu\text{m}$ ;  $t(7) = 8.287$ ,  $p < 0.001$ ) and 3.78 % (virgin:  $3768.93 \pm 19.86 \mu\text{m}$ ; aged:  $3626.40 \pm 33.34 \mu\text{m}$ ;  $t(7) = 3.67$ ,  $p < 0.01$ ), respectively, following 12 months of marine incubation. Biodegradation was the primary pathway of degradation for PCL, supported by extensive modification of the PCL surface, as observed via SEM (Figs. 1, 2), an increase in BET surface area (Fig. 3) and a reduced intensity of IR peaks (SI Fig. 4G). For PVC, the reduction in size was attributed to extensive flaking and cracking of the PVC surface due to photo-oxidative degradation and dechlorination (Fig. 2). While little information exists on the toxicity of the by-products of PCL degradation, the formation of secondary PVC MNPs has significant implications for the health of marine biota due to the carcinogenic and mutagenic impacts associated with phthalate plasticisers and the vinyl chloride monomer<sup>4</sup>.

No difference was observed in the mean diameter of virgin and 12-month aged PP (virgin:  $3462.53 \pm 66.21 \mu\text{m}$ , aged:  $3561.73 \pm 91.97 \mu\text{m}$ ;  $t(7) = -0.88$ ,  $p > 0.1$ ) and PET (virgin:  $2630.15 \pm 26.42 \mu\text{m}$ , aged:  $2632.20 \pm 29.74 \mu\text{m}$ ;  $t(8) = -0.05$ ,  $p > 0.1$ ), suggesting these materials were less susceptible to degradation over the timeframe of ageing.

### Estimating the rate and duration of plastic degradation

Quantitative information on the degradation of plastic polymers is variable and scarce, with estimated timescales spanning several orders of magnitude. Because degradation primarily occurs at the plastic surface, the rate of mass loss is closely related to the surface area of plastic materials<sup>46</sup>. Therefore, we used the particle size measurements obtained via SEM imaging to approximate the rate and duration of degradation for PCL and PVC plastic polymers under natural marine conditions. Degradation rates could not be determined for the remaining plastic polymers due to the small-scale changes in mean particle size over the course of the weathering experiments. We assumed that plastics maintained a constant surface area and followed exponential decay (refer Supplementary Methods 1). Whilst this assumption does not represent the surface changes imparted by long-term marine weathering, it was the most straightforward and comparable way to estimate plastic degradation rates.

Based on the observed changes in mean particle diameter following 12 months of marine ageing, our estimates reveal that the required duration for the degradation of PCL and PVC pellets is 112 and 401 years, respectively (Fig. 7). Previously, surface degradation rates for common plastic polymers (e.g. LDPE, HDPE,

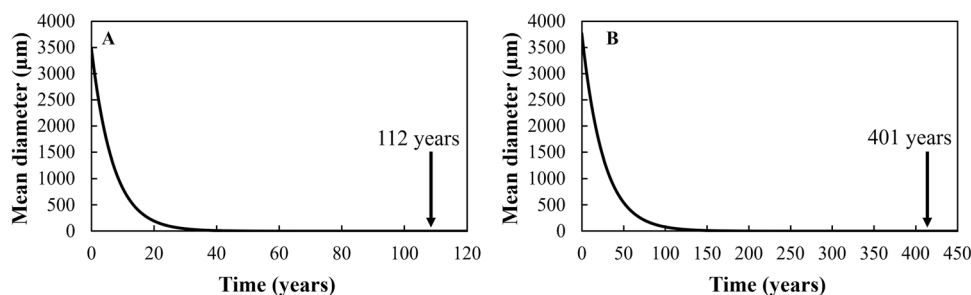


**Fig. 7** Estimated timescale of marine plastic degradation. Panels (A) and (B) represent the time (years) required for PCL and PVC microplastic pellets to degrade in the marine environment in situ.

**Table 2.** Summary of the surface and bulk-phase degradation of 12-month aged marine microplastics and ranking of their marine degradation features.

Polymer Type	Surface artefacts	Surface area	Surface chemistry	Crystallinity (XRD)	Thermal stability	Particle size	Degradation rank
LLDPE	tube worm casts; flaking, cracking; increased surface roughness;	↑ 1265%	↑ C-O	↓ 29.55%	no change	↑ 21.36%	6
PP	flaking, cracking, increased surface roughness, MNP formation	↑ 1202%	↑ C-O; ↓ C=O	↓ 3.79%	no change	no change	4
ePS	(in)organic matter; microbes; marine organisms; PIOM, creases and crevices, increased surface heterogeneity;	↑ 357%	↑ O-H; ↑ C-O	↑ 69.50%	no change	n.d	7
PET	microbes; marine organisms; craters/bubble-like structures, increased surface heterogeneity	↑ 363%	↑ O-H	↓ 19.94%	↓ 8 °C	no change	5
PVC	epiphytes: extensive cracking, flaking, increased surface roughness, MNP formation	↑ 311%	↑ C-O	↓ 18.05%	no change	↓ 3.78%	2
PA	(in)organic matter, biofilms; PIOM, flaking and longitudinal cracks, increased surface heterogeneity	↑ 114%	↑ O-H; ↑ C=O	↓ 23.78%	no change	n.d	3
PCL	pits, cracks, holes, deep fractures and cavities, increased surface roughness and heterogeneity, MNP formation	↑ 765%	↓ C=O; ↓ C-O	↓ 3.06%	no change	↓ 13.46%	1

PP and PET) in marine environments were estimated between 0 and 37  $\mu\text{m}$  per year<sup>46</sup>. Here we provide real-world data that indicates the degradation of plastic surfaces may proceed by more than 12 times current estimates, at a rate of up 469.73  $\mu\text{m}$  per year.

### Marine microplastic degradation

Prolonged immersion of microplastic pellets, foams and fibres in marine surface waters resulted in extensive degradation of plastic surfaces and bulk-phases, which varied by polymer type and time. Overall, weathering led to biofouling, morphological and rheological changes, increased surface area, altered surface chemistry and a decrease in the crystallinity of plastic polymers, with some exceptions. In order to provide a semi-quantitative measure of plastic degradation, the model plastics were ranked from 1 to 7 (highest to lowest) according to the extent of degradation determined by each of the analytical approaches. The extent of degradation was assessed against markers of mechanical, chemical and bio-degradation, with polymers displaying markers of all three degradation pathways receiving a lower rank (greater degradation) than others.

The model bioplastic, PCL, received the highest overall rank (1/7) due to advanced degradation of the plastic surface and a decrease in mean particle diameter (Table 2). Micronanoplastic particles could be seen detaching from the plastic surface, supported by an increase in the BET surface area and reduced intensity of IR peaks, indicative of the loss of low-molecular weight fragments to the environment. PVC displayed the highest level of degradation among common plastic polymers (2/7). Photooxidation in the presence of dissolved inorganic compounds in seawater led to extensive surface degradation and a decrease in mean particle diameter, attributed to the release of potentially toxic MNPs to the environment. Owing to the toxic effects of the vinyl chloride monomer and phthalate plasticisers, the weathering of PVC pellets presents a significant hazard in marine environments. Weathered PA fibres displayed markers of oxidation, hydrolysis and biodegradation, and ranked 3/7 among plastic polymers. Reduced crystallinity and an increase in the concentration of oxygen-containing functional groups was indicative of the degradation of the crystalline coating on PA surfaces and exposure of the amorphous core, suggesting PA may obtain a greater affinity for hydrophobic organic contaminants during the weathering process. No evidence of MNP formation was observed during the 12-month study. Degradation of the PP surface resulted in the loss of low-molecular weight compounds,

including MNPs, to the marine environment. This was supported by a significant increase in BET surface area and a reduction in IR peak intensity corresponding to carbonyl compounds. The presence of chromophoric groups in the virgin material were thought to have initiated extensive photooxidation of the PP surface in what is otherwise considered a relatively resistant polymer to UV exposure. Weathered PET was the only plastic to experience a decrease in thermal stability during marine incubation. This was primarily attributed to microbial degradation, supported by observations of the PET surface and evidence of hydrolytic activity. The degradation of PET in marine environments ranked 5/7 among the model plastics. Long-term weathering led to swelling of LLDPE pellets, evidenced by a significant increase in the mean diameter and surface area of plastic pellets (Table 2). This was attributed to a combination of photooxidation of LLDPE pellets and the diffusion of seawater into the bulk-phase of this low-density polymer. However, without evidence for the formation of plastic degradation products or a reduction in thermal stability, degradation was ranked 6/7 for the model LLDPE.

Finally, in last place (7/7), weathered ePS foam displayed limited evidence of degradation in marine surface waters. While an increase in surface heterogeneity and oxygen containing functional groups were suggestive of surface degradation, the dramatic increase in crystalline content pointed to the high affinity of ePS surfaces for dissolved compounds and PIOM. Remnants of PIOM trapped by the complex surface morphology and high hydrophobicity of ePS foams can contain polar and non-polar compounds, including silica and dissolved metal(loid)s, thereby increasing the concentration of crystalline moieties. This was further supported by the lack of evidence for the formation of plastic degradation products or reduced thermal stability of the bulk-phase. Consequently, while the degradation of ePS may be considered low in marine surface waters, the potential for ePS to adsorb toxic metal(loid)s presents a significant hazard in marine environments. Further research is needed to determine the relationship between weathering and chemical adsorption-desorption processes in real environments in order to fully understand the risks associated with marine plastic pollution.

### CONCLUSION AND IMPLICATIONS FOR FUTURE RESEARCH

This study presents an advanced analytical approach to reveal the natural weathering behaviour of plastic polymers in the marine environment. The findings of this study provide critical long-term time-series information on the degradation of mass-produced plastics in the marine environment, demonstrating that the extent



of weathering varied by time and plastic polymer type. This valuable time-series data demonstrates that weathered plastic surfaces host dynamic environments featuring markers of physical, chemical and biodegradation. Primary microplastics increased in surface area and decreased in crystalline content with increased ageing time. Small micronanoplastics formed on the surface of weathered plastics, providing evidence for the formation of secondary MNPs in-situ. Degradation was most pronounced in PCL and PVC pellets, evidenced by transformation of the plastic surfaces and a decrease in mean particle size. Transformation of PCL and PET surfaces by microbes provides further supporting evidence for the biodegradation of polyesters in marine environments. Finally, plastic-associated inorganic and organic matter promoted the adsorption of inorganic compounds to weathered plastic surfaces, having significant implications for the transfer of hazardous chemical substances to marine biota. To understand the real risks of weathered plastics, further research is needed to investigate the time-dependent impacts of weathering on the leaching of plastic degradation products in different environmental matrices, to determine the potential ecotoxicological risks to human and environmental health. In addition, research and development of alternative plastic materials will help to ensure a precautionary approach to the future management of plastic waste in global oceans.

## METHODS

### Model microplastics

A variety of plastic materials were investigated to determine the impacts of marine weathering on plastic polymers over time. Plastic pre-production pellets, textiles and foam particles ranging between 2500 and 4000  $\mu\text{m}$  in size were obtained from various Australian suppliers, the names of which have been de-identified. Plastic pellets, including linear-low density polyethylene (LLDPE, mean:  $3674.05 \pm 72.25 \mu\text{m}$ ), polypropylene (PP, mean:  $3462.52 \pm 66.21 \mu\text{m}$ ), expanded polystyrene (ePS, mean:  $\sim 3000\text{--}5000 \mu\text{m}$ ), polyethylene terephthalate (PET, mean:  $2630.15 \pm 26.42 \mu\text{m}$ ), and polyvinyl chloride (PVC, mean:  $3768.93 \pm 19.86 \mu\text{m}$ ) were selected according to their global market share and fate as major components of marine debris<sup>1,2</sup>. In addition, aramid textiles (polyaromatic amide, PA, mean:  $\sim 3000\text{--}5000 \mu\text{m}$ ) and polycaprolactone (PCL, mean:  $3489.53 \pm 35.96 \mu\text{m}$ ) pellets were chosen to represent the weathering behaviour of synthetic plastic fibres and biodegradable plastic materials due to their current and projected usage. Detailed information on the physicochemical properties of the selected plastic polymer types is provided in Supplementary Table 3.

### Field sampling

The model plastics were aged in marine surface waters for 12 months, as per the methods described in Supplementary Methods 2. Briefly, ageing units (Supplementary Fig. 9) were deployed in the top 100 cm of the water column across 10 sites in the Hunter Region of NSW, Australia, during October 2018. Subsamples of each material (approx. 1 g, 20–30 pellets) were collected in sterile PP tubes at six time points (0, 1–2, 3–4, 5–6, 8–10 and 12 months) and refrigerated at 4 °C before analysis. Ageing units were inspected for maintenance issues and fouling communities were removed from the outer surface using a wire brush to allow water to flow through freely.

For clean-up, samples were gently rinsed and vortexed in ultrapure water (MilliQ<sup>®</sup>) to remove loosely adhered inorganic and organic matter without damaging the plastic surface and air-dried at room temperature overnight. Finally, samples were pooled by site and allocated for visualisation, surface characterisation and analysis of the bulk phase, to investigate changes in the properties of plastics following long-term marine incubation.

## Material characterisation

Scanning electron microscopy (SEM) was used to investigate small-scale changes in the surface of weathered plastics. Representative samples ( $n = 5$ ) of each plastic type were visualised to measure differences in the size and surface topography of virgin and 12-month aged samples. Samples were mounted on aluminium stubs and coated with a  $\sim 2$  nm platinum layer using a fine auto coater (JEC-3000FC, JEOL). Imaging was performed using a JEOL JSM-7900F SEM operated at an accelerating voltage of 2 kV and a magnification of 100x, 500x, and 1000x for all samples and higher for regions of interest.

Nitrogen adsorption and desorption were analysed using an ASAP 2420 (Micromeritics, USA) surface area and porosity analyser. One gram of virgin and 12-month aged plastic for each polymer type ( $\sim 20\text{--}30$  pellets per sample) were degassed under vacuum ( $p < 1 \times 10^{-5}$ ) for 3 h at 60 °C prior to the adsorption measurements. Due to the low melting temperature of PCL (Supplementary Table 3), degassing was performed for 3 h at 40 °C for virgin and aged samples. The specific surface areas were calculated using the Brunauer–Emmett–Teller (BET) model. However, owing to the complexity of the sample matrix, a significant reduction was observed in the volume of ePS during degassing. Consequently, the BET surface area of ePS was calculated using a single-point analysis as the solid polystyrene beads shrunk while under vacuum.

Attenuated total reflectance fourier transform infrared spectroscopy (ATR-FTIR) (Perkin Elmer FTIR Spectrometer Spectrum Two) was used to investigate differences in the surface chemistry of virgin and aged plastic materials and generate time-series data. Spectra were recorded in reflectance mode in the wavenumber range of 4000–400  $\text{cm}^{-1}$  at a spectral resolution of 4  $\text{cm}^{-1}$  and an average of 8 scans. Representative particles ( $n = 3\text{--}5$  pellets) were selected from each time point and polymer type, and spectra were collected from multiple locations on the particle surface to provide an average spectrum for each sample. Spectra were baseline corrected and normalised, and the hydroxyl, carbonyl and carbon-oxygen indices were calculated for each time point, based on the intensity of O–H (3100–3700  $\text{cm}^{-1}$ ), C=O (1600–1800  $\text{cm}^{-1}$ ) and C–O (1000–1200  $\text{cm}^{-1}$ ) peaks, respectively.

X-ray diffraction (XRD) was used to determine changes in the crystalline structure of the model plastic polymers and generate time-series data. Diffraction patterns for virgin and aged plastics ( $\sim 10\text{--}20$  pellets per sample) were acquired using an Empyrean XRD instrument (Malvern Panalytical, Netherlands), operating with  $\text{CuK}\alpha_1$  and  $\text{K}\alpha_2$  radiations at the wavelength of  $\lambda = 1.5405 \text{ \AA}$  and 1.5444  $\text{ \AA}$  that produce copper radiation using a generator voltage of 40 kV and tube current 40 mA. Samples were scanned between a  $2\theta$  range of 10° to 80° with a step size of 0.006 and time per step of 80 s. Unfortunately, due to sample constraints, we could not generate time-series data for ePS, except virgin and 12-month data.

Differences in thermal stability for virgin and 12-month aged plastic polymers were determined by simultaneous thermogravimetric analysis (TGA) and differential scanning calorimetry (DSC). Analysis was carried out using a Perkin Elmer Thermogravimetric Instrument (STA-8000) to determine the extent of thermal degradation according to changes in the weight percentage, glass transition, and melting temperatures of plastic samples. Samples weighing 10–20 mg were loaded in an alumina crucible and maintained under an  $\text{N}_2$  atmosphere with a flow rate of 50  $\text{mL min}^{-1}$  and a temperature gradient from 30 °C to 800 °C, with a heating rate of 5 °C  $\text{min}^{-1}$ .

Percent crystallinity (%) was estimated using FTIR, XRD, and DSC data for virgin and aged plastics. Briefly, IR bands corresponding to crystalline and amorphous domains were collated from the existing literature and used to calculate percent crystallinity,

following the method described by Zerbi, Gallino<sup>63</sup>;

$$\text{Crystallinity (\%)} = 100 - (1 - I_c/I_a)/1.233 + I_c/I_a * 100 \quad (1)$$

where the intensity ( $I$ ) of  $c$  and  $a$  are determined by the crystalline and amorphous bands (refer Supplementary Fig. 10) and 1.233 corresponds to the theoretical intensity ratio of  $I_c/I_a$  for fully crystalline materials. Similarly, percent crystallinity (%) was calculated from XRD data following the method described by Segal, Creely<sup>64</sup>:

$$\text{Crystallinity (\%)} = I_c/(I_c + I_a) * 100 \quad (2)$$

where  $I_c$  and  $I_a$  are the integrated intensities of crystalline and amorphous phases. Finally, the crystallinity of the model plastics was determined by DSC as the ratio of the peak area of the first enthalpy of fusion ( $\Delta H_m$ ) (J/g) with that of the 100% crystalline plastic reference material ( $\Delta H_{m,0}$ ) (J/g) (available online), to yield an estimate of percent crystallinity for the individual plastic polymers, following the method described by Andrady<sup>27</sup>:

$$\text{Crystallinity (\%)} = (\Delta H_m/\Delta H_{m,0}) * 100 \quad (3)$$

The results obtained from the three approaches were compared to determine their suitability to assess structural changes in the crystallinity of plastics weathered in marine environments over time.

### Particle size measurements

SEM images were further analysed to quantify the extent of surface degradation (%) of plastic pellets in response to marine weathering forces. Differences in the mean size of virgin ( $n = 5$ ) and 12 month-aged ( $n = 5$ ) plastics were determined using the approach described in Supplementary Fig. 11.

### Data analysis

The experimental datasets, tables and analysis were constructed and carried out in Microsoft Excel. All figures were produced in Microsoft Excel and Powerpoint. A series of two samples two-tailed  $t$  tests assuming unequal variance were performed in Microsoft Excel, to test for significant differences in the mean diameter of virgin ( $n = 5$ ) and 12-month-aged ( $n = 5$ ) plastic pellets at the conclusion of the weathering experiments ( $\alpha \leq 0.05$ ).

### DATA AVAILABILITY

The data supporting the main findings are available within the manuscript and supplementary information. Additional supporting data can be obtained from the corresponding author upon reasonable request.

Received: 25 August 2022; Accepted: 7 July 2023;

Published online: 26 July 2023

### REFERENCES

- Geyer, R., Jambeck, J. R. & Law, K. L. Production, use, and fate of all plastics ever made. *Sci. Adv.* **3**, e1700782 (2017).
- Jambeck, J. R. et al. Plastic waste inputs from land into the ocean. *Sci.* **347**, 768–771 (2015).
- Ostle, C. et al. The rise in ocean plastics evidenced from a 60-year time series. *Nat. Commun.* **10**, 1622 (2019).
- Hahladakis, J. N. et al. An overview of chemical additives present in plastics: Migration, release, fate and environmental impact during their use, disposal and recycling. *J. Hazard. Mater.* **344**, 179–199 (2018).
- Andrady, A. L. Microplastics in the marine environment. *Mar. Pollut. Bull.* **62**, 1596–1605 (2011).
- Stanica-Ezeanu, D. & Matei, D. Natural depolymerization of waste poly(ethylene terephthalate) by neutral hydrolysis in marine water. *Sci. Rep.* **11**, 4431 (2021).
- Fernández-González, V. et al. Impact of weathering on the chemical identification of microplastics from usual packaging polymers in the marine environment. *Anal. Chim. Acta* **1142**, 179–188 (2021).
- Lambert, S. & Wagner, M. Formation of microscopic particles during the degradation of different polymers. *Chemosphere* **161**, 510–517 (2016).
- Kedzierski, M. et al. Threat of plastic ageing in marine environment. Adsorption/desorption of micropollutants. *Mar. Pollut. Bull.* **127**, 684–694 (2018).
- Bhagwat, G. et al. Fingerprinting plastic-associated inorganic and organic matter on plastic aged in the marine environment for a decade. *Environ. Sci. Technol.* **55**, 7407–7417 (2021).
- Napper, I. E. & Thompson, R. C. Environmental deterioration of biodegradable, oxo-biodegradable, compostable, and conventional plastic carrier bags in the sea, soil, and open-air over a 3-year period. *Environ. Sci. Technol.* **53**, 4775–4783 (2019).
- Mammo, F. K. et al. Microplastics in the environment: Interactions with microbes and chemical contaminants. *Sci. Total Environ.* **743**, 140518 (2020).
- Fotopoulou, K. N. & Karapanagioti, H. K. Surface properties of beached plastic pellets. *Mar. Environ. Res.* **81**, 70–77 (2012).
- Teuten, E. L. et al. Potential for plastics to transport hydrophobic contaminants. *Environ. Sci. Technol.* **41**, 7759–7764 (2007).
- Alimi, O. S. et al. Weathering pathways and protocols for environmentally relevant microplastics and nanoplastics: What are we missing? *J. Hazard. Mater.* **423**, 126955 (2022).
- Bhagwat, G. et al. Exploring the composition and functions of plastic microbiome using whole-genome sequencing. *Environ. Sci. Technol.* **55**, 4899–4913 (2021).
- Kurata, N. et al. Surfactant-associated bacteria in the near-surface layer of the ocean. *Sci. Rep.* **6**, 19123 (2016).
- Gao, R. & Sun, C. A marine bacterial community capable of degrading poly(ethylene terephthalate) and polyethylene. *J. Hazard. Mater.* **416**, 125928 (2021).
- Zettler, E. R., Mincer, T. J. & Amaral-Zettler, L. A. Life in the 'plastisphere': microbial communities on plastic marine debris. *Environ. Sci. Technol.* **47**, 7137–7146 (2013).
- Pascall, M. A. et al. Uptake of polychlorinated biphenyls (PCBs) from an aqueous medium by polyethylene, polyvinyl chloride, and polystyrene films. *J. Agric. Food Chem.* **53**, 164–169 (2005).
- George, S. C. & Thomas, S. Transport phenomena through polymeric systems. *Prog. Polym. Sci.* **26**, 985–1017 (2001).
- Fernández-González, V. et al. Misidentification of PVC microplastics in marine environmental samples. *TrAC, Trends Anal. Chem.* **153**, 116649 (2022).
- Corcoran, P. L., Biesinger, M. C. & Grifi, M. Plastics and beaches: A degrading relationship. *Mar. Pollut. Bull.* **58**, 80–84 (2009).
- Gewert, B. et al. Identification of chain scission products released to water by plastic exposed to ultraviolet light. *Environ. Sci. Technol.* **5**, 272–276 (2018).
- Carbery, M., O'Connor, W. & Palanisami, T. Trophic transfer of microplastics and mixed contaminants in the marine food web and implications for human health. *Environ. Int.* **115**, 400–409 (2018).
- Jäms, I. B. et al. Estimating the size distribution of plastics ingested by animals. *Nat. Commun.* **11**, 1594 (2020).
- Andrady, A. L. The plastic in microplastics: A review. *Mar. Pollut. Bull.* **119**, 12–22 (2017).
- Puttonen, T., Salmi, M. & Partanen, J. Mechanical properties and fracture characterization of additive manufacturing polyamide 12 after accelerated weathering. *Polym. Test.* **104**, 107376 (2021).
- Agboola, O. D. & Benson, N. U. Physisorption and chemisorption mechanisms influencing micro (nano) plastics-organic chemical contaminants interactions: A review. *Front. Environ. Sci.* **9**, 1–27 (2021).
- Jung, M. R. et al. Validation of ATR FT-IR to identify polymers of plastic marine debris, including those ingested by marine organisms. *Mar. Pollut. Bull.* **127**, 704–716 (2018).
- Elzein, T. et al. FTIR study of polycaprolactone chain organization at interfaces. *J. Colloid Interface Sci.* **273**, 381–387 (2004).
- Wang, W., Wang, S.-X. & Guan, H.-S. The antiviral activities and mechanisms of marine polysaccharides: An overview. *Mar. Drugs* **10**, 2795–2816 (2012).
- Su, X. et al. Estuarine plastisphere as an overlooked source of N<sub>2</sub>O production. *Nat. Commun.* **13**, 3884 (2022).
- Brandon, J., Goldstein, M. & Ohman, M. D. Long-term aging and degradation of microplastic particles: Comparing in situ oceanic and experimental weathering patterns. *Mar. Pollut. Bull.* **110**, 299–308 (2016).
- Samper, M. D. et al. Recycling of expanded polystyrene from packaging. *Prog. Rubber Plast. Recycl. Technol.* **26**, 83–92 (2010).
- Gewert, B., Plassmann, M. M. & MacLeod, M. Pathways for degradation of plastic polymers floating in the marine environment. *Environ. Sci.: Process. Impacts* **17**, 1513–1521 (2015).
- Derombise, G. et al. Degradation of aramid fibers under alkaline and neutral conditions: Relations between the chemical characteristics and mechanical properties. *J. Appl. Polym. Sci.* **116**, 2504–2514 (2010).
- Nascimento, R. F. et al. Influence of UV radiation and moisture associated with natural weathering on the ballistic performance of aramid fabric armor. *J. Mater. Res. Technol.* **9**, 10334–10345 (2020).

39. Min, K., Cuiffi, J. D. & Mathers, R. T. Ranking environmental degradation trends of plastic marine debris based on physical properties and molecular structure. *Nat. Commun.* **11**, 727 (2020).
40. Mohanan, N. et al. Microbial and enzymatic degradation of synthetic plastics. *Front. Microbiol.* **11**, 580709 (2020).
41. Fotopoulou, K. N. & Karapanagioti, H. K. Degradation of Various Plastics in the Environment in Hazardous Chemicals Associated with Plastics in the Marine Environment. Springer International Publishing. 71–92 (2019).
42. Tsuji, H. & Ikada, Y. Blends of aliphatic polyesters. II. Hydrolysis of solution-cast blends from poly(L-lactide) and poly(E-caprolactone) in phosphate-buffered solution. *J. Appl. Polym. Sci.* **67**, 405–415 (1998).
43. Wang, G.-X. et al. Seawater-degradable polymers—fighting the marine plastic pollution. *Adv. Sci.* **8**, 2001121 (2021).
44. Yousif, E. & Hasan, A. Photostabilization of poly(vinyl chloride) – Still on the run. *J. Taibah Univ. Med. Sci.* **9**, 421–448 (2015).
45. Rani, M. et al. Qualitative analysis of additives in plastic marine debris and its new products. *Arch. Environ. Contam. Toxicol.* **69**, 352–366 (2015).
46. Chamas, A. et al. Degradation rates of plastics in the environment. *ACS Sustain. Chem. Eng.* **8**, 3494–3511 (2020).
47. Yousif, E. & Haddad, R. Photodegradation and photostabilization of polymers, especially polystyrene: review. *Springerplus* **2**, 398 (2013).
48. Leonas, K. K. The disintegration rate of traditional and chemically modified plastic films in simulated fresh-and sea-water environments. *J. Appl. Polym. Sci.* **47**, 2103–2110 (1993).
49. Chew, S. C. & Yang, L. *Biofilms in Encyclopedia of Food and Health*. Oxford Academic Press. 407–415 (2016).
50. Lambert, S. & Wagner, M. *Microplastics Are Contaminants of Emerging Concern in Freshwater Environments: An Overview in Freshwater Microplastics: Emerging Environmental Contaminants?* Springer International Publishing. 1–23 (2018).
51. Li, H. et al. The role of thermo-oxidative aging at different temperatures on the crystal structure of crosslinked polyethylene. *J. Mater. Sci. Mater. Electron.* **29**, 3696–3703 (2018).
52. Turner, A. Polystyrene foam as a source and sink of chemicals in the marine environment: An XRF study. *Chemosphere* **263**, 128087 (2021).
53. Fu, Q. et al. Mechanism analysis of heavy metal lead captured by natural-aged microplastics. *Chemosphere* **270**, 128624 (2021).
54. Pinto, M. et al. The composition of bacterial communities associated with plastic biofilms differs between different polymers and stages of biofilm succession. *PLoS One* **14**, e0217165 (2019).
55. Paluselli, A. et al. Phthalate release from plastic fragments and degradation in seawater. *Environ. Sci. Technol.* **53**, 166–175 (2019).
56. Chen, Y. et al. Catalytic dechlorination and charring reaction of polyvinyl chloride by CuAl layered double hydroxide. *Energy Fuels* **32**, 2407–2413 (2018).
57. López, A. et al. Dechlorination of fuels in pyrolysis of PVC containing plastic wastes. *Fuel Process. Technol.* **92**, 253–260 (2011).
58. Beyler, C. L. & Hirschler, M. M. Thermal decomposition of polymers. *SFPE handbook of fire protection engineering*. **2**, (2002).
59. Arp, H. P. H. et al. Weathering plastics as a planetary boundary threat: Exposure, fate, and hazards. *Environ. Sci. Technol.* **55**, 7246–7255 (2021).
60. Müller, A. et al. The effect of polymer aging on the uptake of fuel aromatics and ethers by microplastics. *Environ. Pollut.* **240**, 639–646 (2018).
61. ter Halle, A. et al. To what extent are microplastics from the open ocean weathered? *Environ. Pollut.* **227**, 167–174 (2017).
62. Chun, K. S., Husseinsyah, S. & Syazwani, N. F. Properties of kapok husk-filled linear low-density polyethylene ecomposites: Effect of polyethylene-grafted acrylic acid. *J. Thermoplast. Compos. Mater.* **29**, 1641–1655 (2016).
63. Zerbi, G. et al. Structural depth profiling in polyethylene films by multiple internal reflection infra-red spectroscopy. *Polymer* **30**, 2324–2327 (1989).
64. Segal, L. et al. An empirical method for estimating the degree of crystallinity of native cellulose using the X-ray diffractometer. *Text. Res. J.* **29**, 786–794 (1959).
65. Brandon, J. A., Jones, W. & Ohman, M. D. Multidecadal increase in plastic particles in coastal ocean sediments. *Sci. Adv.* **5**, eaax0587 (2019).
66. Cai, L. et al. Observation of the degradation of three types of plastic pellets exposed to UV irradiation in three different environments. *Sci. Total Environ.* **628–629**, 740–747 (2018).
67. Nel, H. A. et al. An untargeted thermogravimetric analysis-fourier transform infrared-gas chromatography-mass spectrometry approach for plastic polymer identification. *Environ. Sci. Technol.* **55**, 8721–8729 (2021).

## ACKNOWLEDGEMENTS

This work was supported by University of Newcastle Australia through the 50/50 Industry Scholarship in partnership with the City of Newcastle, NSW [G1601286]. The authors wish to thank Dr. Joseph Stalin for his expertise and assistance with thermal analysis techniques.

## AUTHOR CONTRIBUTIONS

M.C., C.I.S. and T.P. conceptualized the project. W.O. provided valuable field resources and scientific advice. M.C. planned and executed the field sampling. M.C. and L.D. processed the samples in the laboratory. M.C. and C.I.S. performed the FTIR, XRD, BET, SEM and TGA-DSC analyses and interpreted the data. M.C. prepared the manuscript draft. C.I.S. participated in valuable discussions and provided useful feedback during manuscript preparation. T.P. led the research program. All authors contributed to reviewing of the final manuscript.

## COMPETING INTERESTS

The authors declare no competing interests.

## ADDITIONAL INFORMATION

**Supplementary information** The online version contains supplementary material available at <https://doi.org/10.1038/s41529-023-00377-y>.

**Correspondence** and requests for materials should be addressed to Palanisami Thava.

**Reprints and permission information** is available at <http://www.nature.com/reprints>

**Publisher's note** Springer Nature remains neutral with regard to jurisdictional claims in published maps and institutional affiliations.



**Open Access** This article is licensed under a Creative Commons Attribution 4.0 International License, which permits use, sharing, adaptation, distribution and reproduction in any medium or format, as long as you give appropriate credit to the original author(s) and the source, provide a link to the Creative Commons license, and indicate if changes were made. The images or other third party material in this article are included in the article's Creative Commons license, unless indicated otherwise in a credit line to the material. If material is not included in the article's Creative Commons license and your intended use is not permitted by statutory regulation or exceeds the permitted use, you will need to obtain permission directly from the copyright holder. To view a copy of this license, visit <http://creativecommons.org/licenses/by/4.0/>.

© The Author(s) 2023